ACS Catalysis

pubs.acs.org/acscatalysis Research Article

# Identification of a Facile Pathway for Dioxymethylene Conversion to Formate Catalyzed by Surface Hydroxyl on $TiO_2$-Based Catalyst

Xueyan Chen,[‖] Guangzhi He,[‖] Yaobin Li, Min Chen, Xiaoxiao Qin, Changbin Zhang,* and Hong He

Cite This: *ACS Catal.* 2020, 10, 9706−9715 Read Online

**ABSTRACT:** Formaldehyde (HCHO) is either a reactant, intermediate, or product in numerous industrial catalytic reactions; therefore, revealing the full transformation process of HCHO during heterogeneous catalysis is of prime importance in understanding the mechanisms of many HCHO-related reactions and designing more efficient catalysts. As two main intermediates in HCHO transformation, the conversion of dioxymethylene (DOM) to formate is one of the key steps. There are three recognized pathways for this step, including direct dissociation of DOM, DOM combining with surface O, or through a Cannizzaro-type reaction. Herein, we reveal that the catalytic reaction between DOM and the abundant surface OH groups is a facile pathway for the transformation of DOM to formate species on $TiO_2$ and also on $TiO_2$-supported noble metal catalysts. In situ diffuse reflectance infrared Fourier transform spectroscopy (DRIFTS) results demonstrate that the presence of water vapor is favorable for the conversion of DOM to formate species on $TiO_2$, and the loading of noble metals (Ir/Pt) on $TiO_2$ further promotes the activation of $H_2O$, thereby boosting the transformation of DOM into formate. Density functional theory (DFT) calculations show that HCHO consumes the bridging OH groups to form DOM species first followed by the reaction between DOM and the terminal OH groups on the $TiO_2$ surface to produce formate, and the latter reaction is both thermodynamically and kinetically favorable. These results provide deeper insight into HCHO transformation and demonstrate another role of surface hydroxyl groups in catalytic reaction.

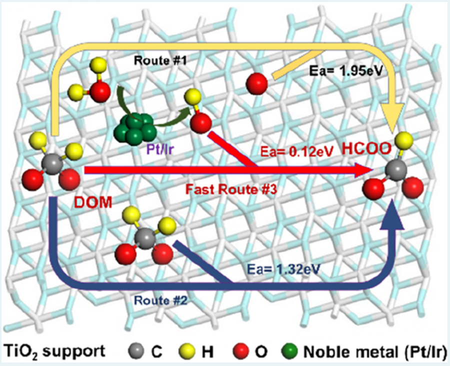

**KEYWORDS:** *hydroxyl, dioxymethylene (DOM), formate, metal oxide surface, promotion effect*

## INTRODUCTION

Formaldehyde (HCHO) is the simplest aldehyde, and it or its adsorbed forms is either a reactant, product, or key intermediate in numerous important industrial catalytic reactions such as methanol oxidation,[1] methyl formate production,[2] methanol dehydrogenation, and synthesis[3,4] as well as higher alcohol and Fischer−Tropsch syntheses.[5,6] Hence, HCHO is often employed as a probe molecule to investigate the adsorption and reaction behavior of the aldehyde groups or $C_1$ molecules on solid surfaces.[7] Beyond this, gaseous HCHO is known to be a harmful indoor air pollutant leading to serious health problems, and its destruction by catalytic oxidation under ambient conditions is the most efficient technology for indoor air HCHO elimination.[8] It is of great interest to identify the full adsorption and reaction pathway of HCHO on catalyst surfaces to understand the mechanisms of industry-relevant catalytic reactions and to guide the design of more efficient catalysts for HCHO oxidation.

Many studies have been carried out concerning the adsorption and transformation processes of HCHO on metal surfaces such as Cu (110) and Pt (111) and also on metal oxides such as $TiO_2$, $SiO_2$, $Al_2O_3$, and so on.[6,9−13] It is generally believed that dioxymethylene (DOM, $H_2CO_2$) and formate species (HCOO) are the primary intermediates for HCHO transformation, and the structural formulas of which are shown in Figure S1. In the initial step, HCHO can react with the surface O species or OH groups to form DOM species.[6,9,10,14−16] There are three recognized pathways for the formation of formate species from DOM. The first pathway is the direct dissociation of DOM to produce HCOO on a metal surface in the absence of O atoms.[9] When oxygen species exist on the surface, DOM has a propensity to combine with surface oxygen to form formate species, which is the second pathway for transformation of DOM.[16−19] The third pathway involves a Cannizzaro-type reaction in which the DOM is disproportionated into a formate species and a methoxide group due to hydride transfer between two DOM species.[6,20] There are two main routes for the further transformation of formate species. When the catalyst has sufficient capacity for $H_2O$ activation to hydroxyl groups, the direct oxidation mechanism of HCOO +

**Received:** April 29, 2020
**Revised:** July 31, 2020
**Published:** July 31, 2020

https://dx.doi.org/10.1021/acscatal.0c01901

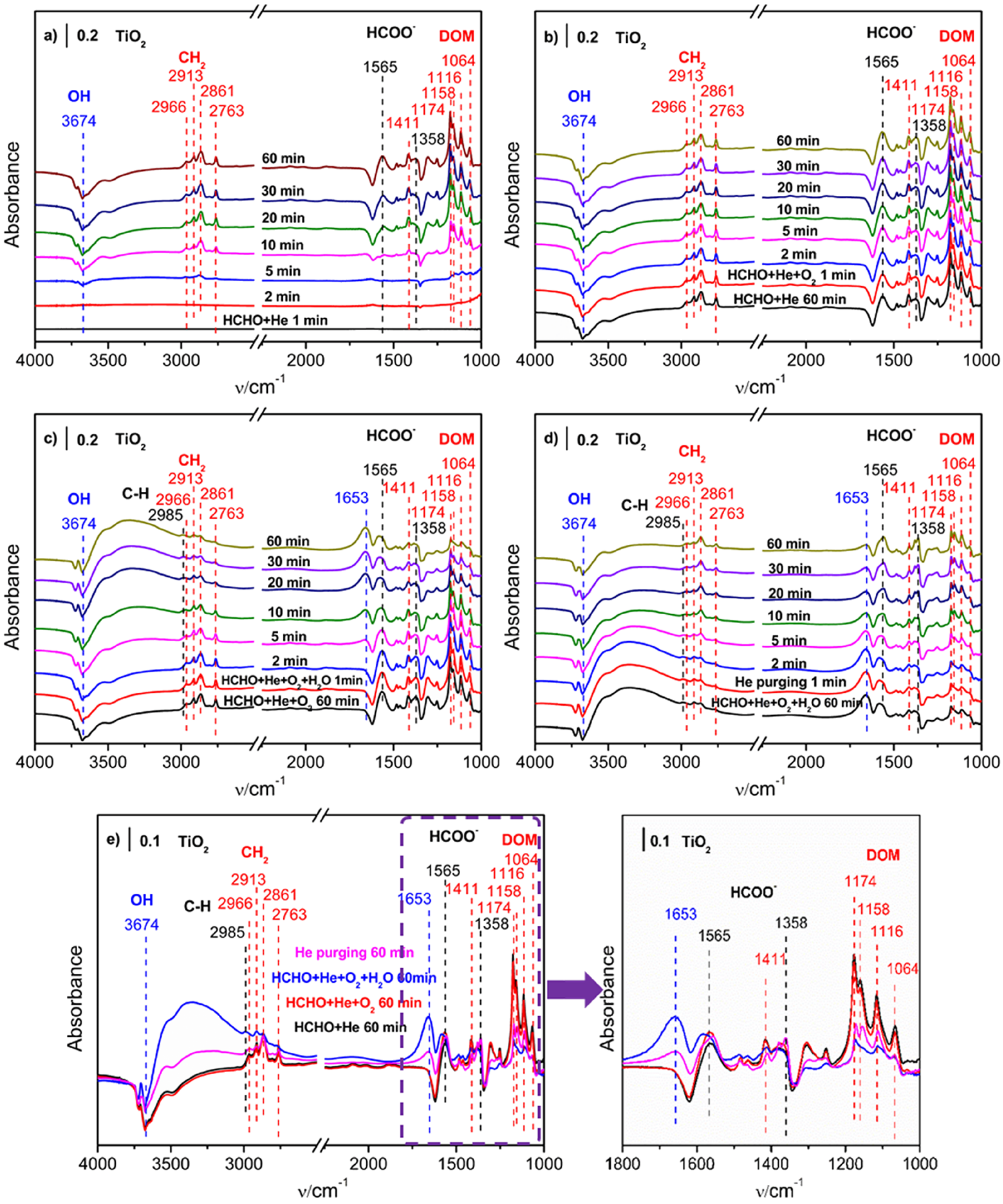

**Figure 1.** Dynamic changes of in situ DRIFTS of the $TiO_2$ sample in a flow of (a) HCHO + He for 60 min, followed by (b) HCHO + He + $O_2$ for 60 min, then (c) HCHO + He + $O_2$ + $H_2O$ for 60 min, and finally by (d) He purging for 60 min. (e) Spectra at a steady state at room temperature. Reaction conditions: 120 ppm HCHO, 20% $O_2$, 35% RH, He balance, and a total flow rate of 100 cm$^3$ min$^{-1}$.

OH → $H_2O$ + $CO_2$ takes place;[21−23] otherwise, the formate species decompose into adsorbed CO species first, and the CO species then react with $O_2$ to produce gas-phase $CO_2$ (HCOO → CO → $CO_2$).[14,24−26]

As previously reported, water can be dissociated into surface OH groups on oxygen vacancies[27,28] or on metal surfaces through water−oxygen interactions.[29,30] Surface hydroxyl is a well-known active oxygen species, which plays an extensive role in various photochemical and catalytic reactions.[21−23,31−38] It has been shown that OH groups can facilitate the adsorption and diffusion of $O_2$ on Au/$TiO_2$[33] and also that the concentration of surface OH groups influences the dispersion of active metal on the support, thus affecting the catalytic activity of catalysts.[34,35] Our previous works[21,23,31] and a number of other studies[22,36,37] have demonstrated that surface OH groups play a key role in the catalytic oxidation of HCHO, and the presence of water vapor can greatly improve the efficiencies of catalysts for HCHO oxidation, which have been mainly related to the fact that the abundant OH groups on the catalyst surface can significantly favor the conversion of formate to $H_2O$ and $CO_2$.

In this work, we carefully investigated HCHO adsorption and transformation in the presence and absence of $O_2$ and $H_2O$ on pristine $TiO_2$ and $TiO_2$-supported noble metal (Pt and Ir) catalysts using in situ diffuse reflectance infrared Fourier transform spectroscopy (DRIFTS) experiments and DFT calculations. We observe that the presence of $H_2O$ can promote the conversion of DOM to formate species on $TiO_2$, and the promotion effect is more pronounced when noble metals are loaded on $TiO_2$. DFT calculation results show that surface OH species can catalyze DOM to form formate species on $TiO_2$ surfaces, and the loading of Pt or Ir on $TiO_2$ promotes the dissociation of $H_2O$ to surface OH groups, therefore greatly enhancing the transformation of DOM to formate. Our

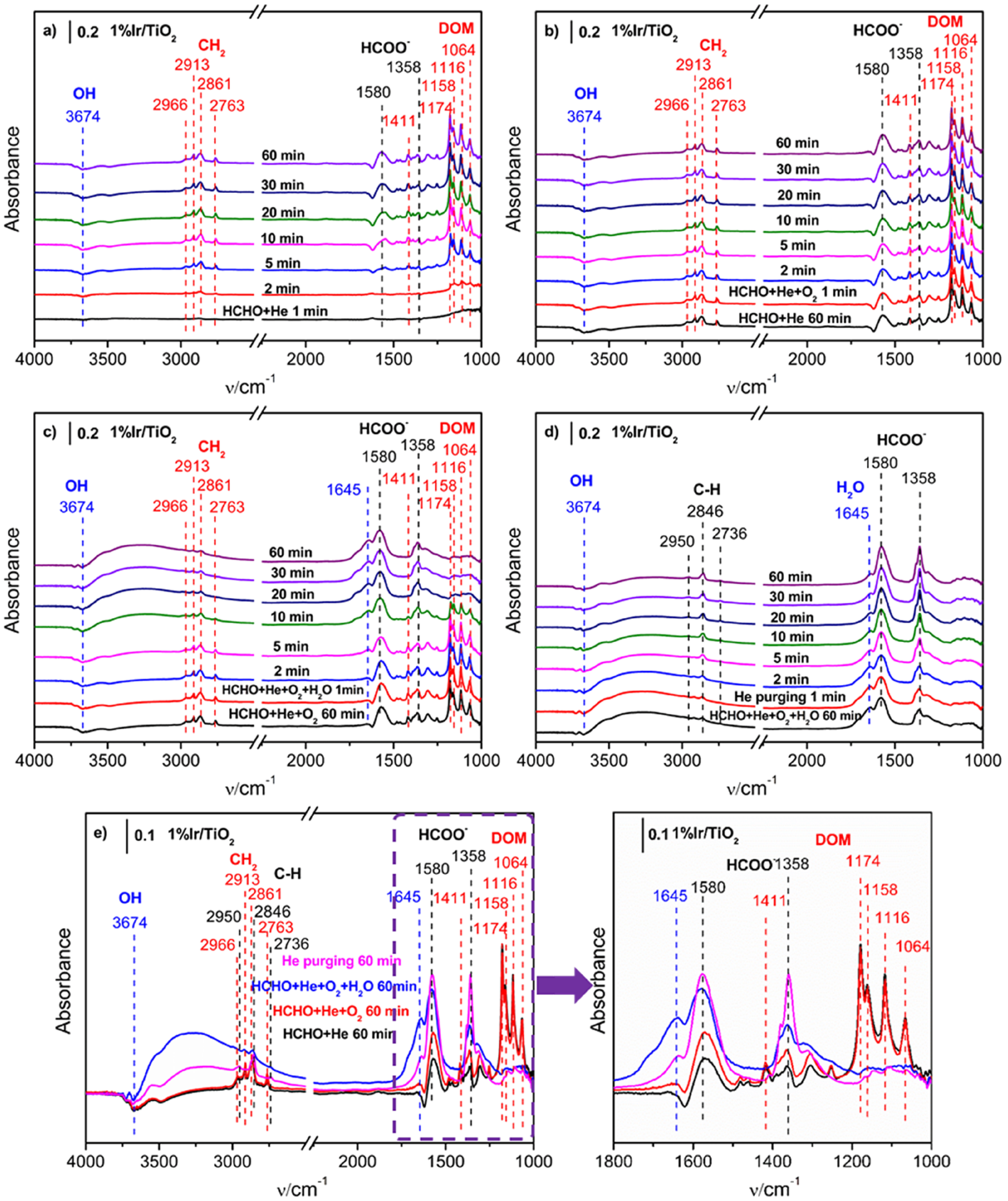

Figure 2. Dynamic changes of in situ DRIFTS of the Ir/$TiO_2$ sample in a flow of (a) HCHO + He for 60 min, followed by (b) HCHO + He + $O_2$ for 60 min, then (c) HCHO + He + $O_2$ + $H_2O$ for 60 min, and finally by (d) He purging for 60 min. (e) Spectra at a steady state at room temperature. Reaction conditions: 120 ppm HCHO, 20% $O_2$, 35% RH, He balance, and a total flow rate of 100 $cm^3$ $min^{-1}$.

findings demonstrate that the reaction between DOM and OH is a new and facile pathway for the transformation of DOM into formate species.

## ■ RESULTS AND DISCUSSION

**In Situ DRIFTS of HCHO Adsorption and Transformation on $TiO_2$.** In situ DRIFTS experiments were performed to investigate HCHO adsorption and transformation in the presence and absence of $O_2$ and $H_2O$ on pristine $TiO_2$. The dynamic and steady-state in situ DRIFTS spectra are presented in Figure 1. After exposing the $TiO_2$ to a flow of HCHO + He for 60 min, the bands at 1064, 1116, 1158, 1174, 1358, 1411, 1565, 2763, 2861, 2913, 2966, and 3674 $cm^{-1}$ appear (Figure 1a). The bands at 1064, 1116, 1158, 1174, and 1411 $cm^{-1}$ are ascribed to $\nu$(C−O) and $\omega(CH_2)$ in DOM species, and the bands at 2763, 2861, 2913, and 2966 $cm^{-1}$ are ascribed to $\nu(CH_2)$ of DOM.[6,11,15] The very weak bands appearing at 1358 and 1565 $cm^{-1}$ are assigned to the symmetric stretch $\nu_s$ ($COO^-$) and the asymmetric stretch $\nu_{as}$ ($COO^-$) of formate.[39] A negative peak at 3674 $cm^{-1}$ related to surface bridging hydroxyl (OH) species is also clearly detected with HCHO adsorption.[40] These results show that HCHO is mainly converted to adsorbed DOM species on $TiO_2$ by consuming bridging hydroxyl groups on the surface in the flow of HCHO + He, and only a small portion of DOM are transformed to formate.[16,18] No peaks related to molecularly adsorbed HCHO, formic acid,[15,24] or the methoxide group[6] are observed on the $TiO_2$ surface.

Subsequently, $O_2$ is added to the gas flow in the system. After exposing the system to a flow of HCHO + He + $O_2$ for 60 min, there is no observable change in the peak intensities of DOM and $HCOO^-$ species (Figure 1b), indicating that $O_2$ has no influence on DOM formation and conversion on $TiO_2$. When water vapor is introduced into the system (Figure 1c),

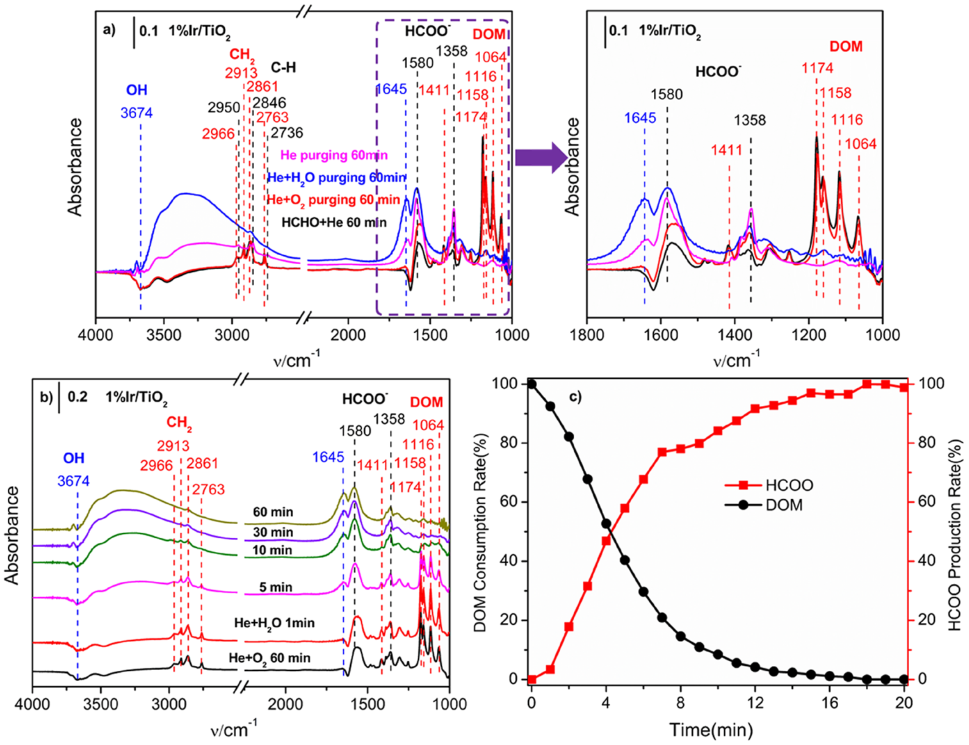

**Figure 3.** (a) In situ DRIFTS spectra over Ir/$TiO_2$ in a flow of HCHO + He for 60 min (1), followed by He + $O_2$ for 60 min (2), then He + $H_2O$ for 60 min (3), and finally by He purging for 60 min (4). (b) Dynamic changes of in situ DRIFTS of the Ir/$TiO_2$ sample in a flow of He + $H_2O$ for 60 min at room temperature with (c) changes in the band areas of the DOM and formate species (HCOO: 1492−1660 $cm^{-1}$; DOM: 1012−1220 $cm^{-1}$) over time. Reaction conditions: 120 ppm HCHO, 20% $O_2$, 35% RH, He balance, and a total flow rate of 100 $cm^3$ $min^{-1}$.

the peak intensities of both DOM and $HCOO^-$ species clearly decrease. After subsequently purging with He for 60 min (Figure 1d), the intensity of the peak at 1653 $cm^{-1}$ related to water sharply drops and the peak intensities of DOM species are partially recovered, indicating that water may cover the adsorbed surface species, thereby decreasing the related peak intensities. Importantly, after final purging with He, we observe that the peak intensities of formate species (1358 and 1565 $cm^{-1}$) are slightly increased, while those of DOM species are decreased compared with their initial states (Figure 1e), demonstrating that some DOM are transformed into formate species by the interaction with water vapor. Taking the above findings into account, we conclude that the presence of water vapor promotes the conversion of DOM to formate on $TiO_2$, and the reaction of DOM with surface hydroxyl groups may be a new pathway for DOM transformation.

**In Situ DRIFTS of HCHO Adsorption and Transformation on Ir/$TiO_2$.** It is known that noble metals have the stronger ability to activate $O_2$ and $H_2O$ than ordinary metal oxides. We next loaded different noble metals such as Ir and Pt on $TiO_2$ and further investigated the adsorption and transformation behaviors of DOM and HCOO species. Figure 2 presents the dynamic and steady-state in situ DRIFTS spectra over the Ir/$TiO_2$ sample. After Ir/$TiO_2$ is exposed to a flow of HCHO + He for 60 min (Figure 2a), DOM and HCOO species are also formed on Ir/$TiO_2$. Similar to the results on $TiO_2$, the DOM species are dominant on the surface, and the formate species remain at a low concentration level. When $O_2$ is added into the system, the peak intensities of DOM and $HCOO^-$ remain almost unchanged in the flow of HCHO + He + $O_2$ for 60 min (Figure 2b), confirming that $O_2$ is still inactive for DOM conversion, even on Ir/$TiO_2$. After water vapor is introduced (Figure 2c), the peak intensities of DOM species sharply drop and the peaks of formate species quickly build up. The DOM species completely disappear within 20 min on Ir/$TiO_2$ in the flow of He + HCHO + $O_2$ + $H_2O$. After subsequently purging with He for 60 min (Figure 2d), we can clearly observe that the formate species ($\nu_s$ ($COO^-$) 1358 $cm^{-1}$, $\nu_{as}$ ($COO^-$) 1580 $cm^{-1}$, and $\nu$(C−H) 2736, 2846, and 2950 $cm^{-1}$) are dominant on the Ir/$TiO_2$ catalyst surface. These findings confirm that Ir loading on $TiO_2$ greatly improves the $H_2O$ activation, therefore significantly promoting the transformation of DOM into formate.

To eliminate the possible effects of oxygen coexistence with water vapor and to confirm the role of $H_2O$ in DOM transformation, we changed the entry order of oxygen and water vapor (shown in Figure S4). We first introduce water vapor into the gas flow after the Ir/$TiO_2$ sample is exposed to a flow of HCHO + He for 60 min. As expected, the DOM species still quickly disappear in 20 min and are converted into formate species in the presence of water vapor (Figure S4b). We next investigated the transformation of the adsorbed DOM species on the Ir/$TiO_2$ sample in the absence of HCHO. As Figure 3a shows, after exposing the Ir/$TiO_2$ to a flow of HCHO + He for 60 min, adsorbed DOM species are formed. We next stop the HCHO flow to measure the reactivity of the adsorbed DOM species toward $O_2$ or $H_2O$. As we can see, the introduction of $O_2$ does not induce obvious changes in the spectra, and when water vapor is switched into the system, the band intensities for DOM species decrease along with the increase of those for formate species (Figure 3a,b). The peak areas of the DOM and formate species (HCOO: 1492−1660 $cm^{-1}$; DOM: 1012−1220 $cm^{-1}$) in Figure 3b were integrated and displayed as a function of time in Figure 3c. It is clear that

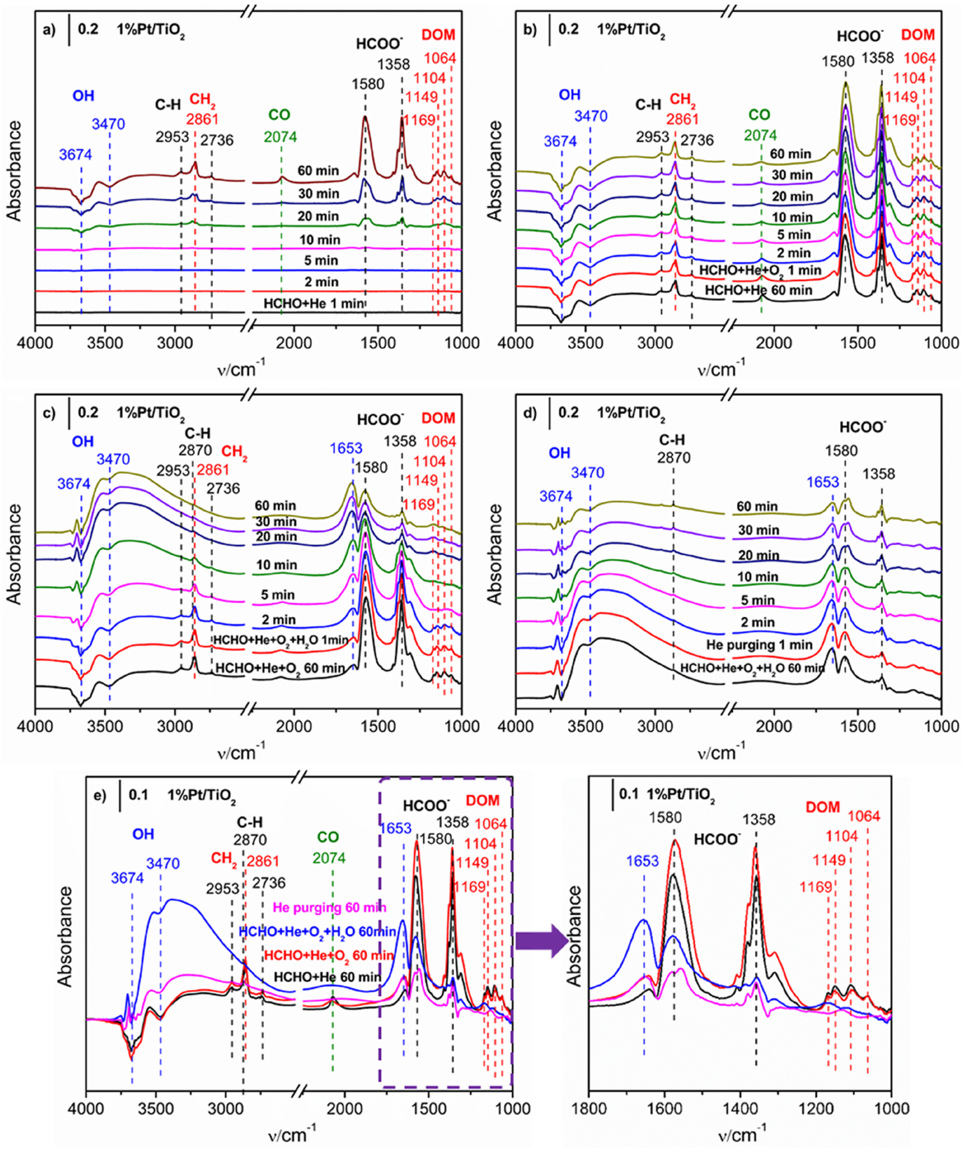

**Figure 4.** Dynamic changes of in situ DRIFTS of the Pt/TiO$_2$ sample in a flow of (a) HCHO + He for 60 min, followed by (b) HCHO + He + O$_2$ for 60 min, then (c) HCHO + He + O$_2$ + H$_2$O for 60 min, and finally by (d) He purging for 60 min. (e) Spectra at a steady state at room temperature. Reaction conditions: 120 ppm HCHO, 20% O$_2$, 35% RH, He balance, and a total flow rate of 100 cm$^3$ min$^{-1}$.

the surface DOM species completely disappear in 20 min and transform into formate species on Ir/TiO$_2$ in the flow of He + H$_2$O. In addition, we do not observe any other species such as methoxy groups, formic acid, or methanol on the Ir/TiO$_2$ surface or in the reaction atmosphere (shown in Figure S5); therefore, we can confirm that adsorbed DOM is directly oxidized into formate species through interaction with surface OH groups.

**In Situ DRIFTS of HCHO Adsorption and Transformation on Pt/TiO$_2$.** We also conducted the same in situ DRIFTS experiments on the Pt/TiO$_2$ (Figure 4) sample and observed similar experimental phenomena, indicating that water vapor has a common promotion effect on noble metal-based catalysts for the transformation of DOM to formate. Interestingly, some subtle differences can be found in the HCHO transformation processes on Ir/TiO$_2$ and Pt/TiO$_2$ catalysts by comparing the details of the DRIFTS spectra. Figure 2 shows that DOM species are dominant on the Ir/TiO$_2$ catalyst surface in a flow of HCHO + He. In contrast, as shown in Figure 4, when Pt/TiO$_2$ is exposed to HCHO + He for 60 min, formate rather than DOM species are dominant on the Pt/TiO$_2$ surface. In addition, we also observe that the peaks of HCOO species quickly decrease on the Pt/TiO$_2$ catalyst after water vapor is introduced into the gas flow, indicating that the formate species directly react with OH to form CO$_2$ and H$_2$O on Pt/TiO$_2$, which has already been demonstrated in our previous studies.[21]

The above findings suggest that the types, concentrations, and reactivity of surface OH groups are different among the TiO$_2$, Ir/TiO$_2$, and Pt/TiO$_2$ samples, and their capacities for the activation of surface OH groups may be also different from each other, therefore leading to different behaviors in HCHO transformation. We next investigated the types and concentrations of OH groups on TiO$_2$, Ir/TiO$_2$, and Pt/TiO$_2$ by using in situ DRIFTS of NH$_3$ adsorption since NH$_3$ can react with and then consume the surface OH groups during adsorption.[41] As shown in Figure S6, some negative peaks in the range of 3600−3800 cm$^{-1}$ appear due to the consumption

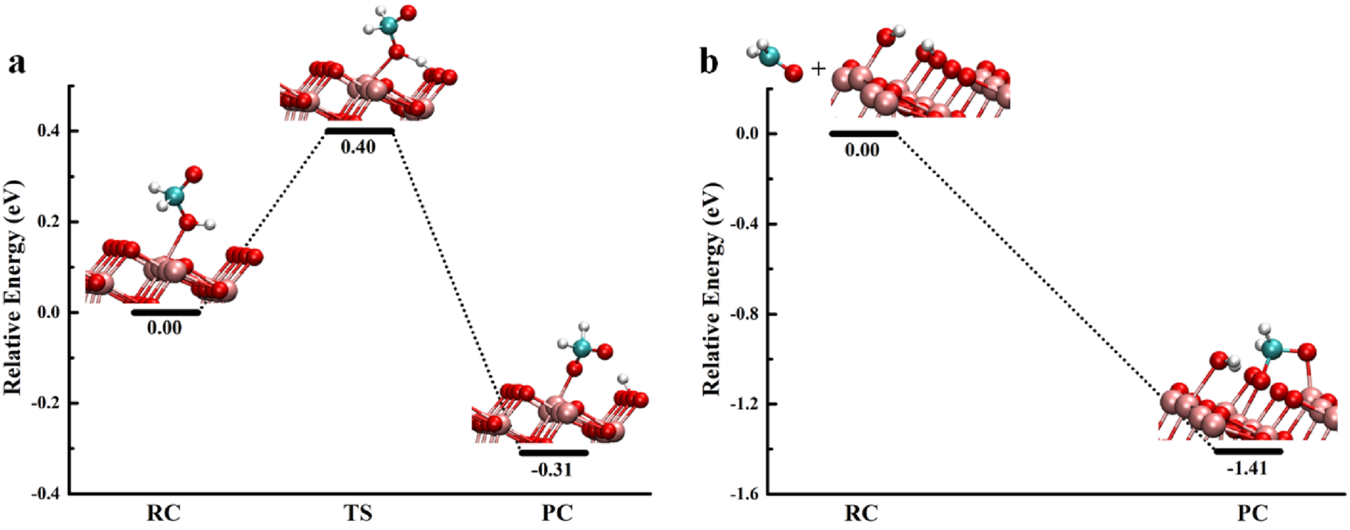

**Figure 5.** Energy profiles of the reaction pathway of DOM ($CH_2O_2$) formation: (a) HCHO adsorption on the terminal OH group; (b) HCHO adsorption on the bridging OH group. Pink, red, cyan, and white circles denote Ti, O, C, and H atoms, respectively.

of surface OH groups. The band at 3731 $cm^{-1}$ is ascribed to isolated terminal OH, and the bands at 3696, 3675, and 3631 $cm^{-1}$ are ascribed to bridging OH.[40,42] It is noted that the types of OH groups on the three samples are similar; the amount of surface OH on $TiO_2$ is almost equal to that on Pt/$TiO_2$ but much higher than that on Ir/$TiO_2$. The loading of Pt and Ir on $TiO_2$ will occupy a portion of the surface OH sites, and the different concentrations of OH groups on Pt/$TiO_2$ and Ir/$TiO_2$ should be related to their different capacities for activating $H_2O$. These results show that the types and concentrations of OH groups are not the key factors inducing their different behaviors in HCHO transformation. Hence, the other two factors, the reactivity of OH groups and their activation, may play the crucial roles in influencing HCHO transformation, which was next investigated by DFT calculations.

**DFT Calculations.** The pathways of HCHO transformation on $TiO_2$ were further determined using density functional theory (DFT) calculations. As shown in Figure 5, an HCHO molecule is first adsorbed on a surface OH group (terminal or bridging), and then, the H atom of the surface OH group transfers to an adjacent surface O or OH group, leading to the formation of dioxymethylene species ($CH_2O_2$, DOM). The formation of DOM on a terminal OH group needs to overcome a barrier of 0.40 eV (Figure 5a). In contrast, it is barrierless for the reaction between HCHO and a surface bridging OH group (Figure 5b), on which HCHO occupies a surface bridging OH group to produce DOM, and the H atom in the bridging OH group bonds with an adjacent terminal OH group, forming molecularly adsorbed $H_2O$ (HCHO + b-OH → $CH_2O_2$). These results indicate that the bridging OH group is much more reactive toward HCHO than the terminal OH group; therefore, it is responsible for DOM formation. These findings are in good agreement with the in situ DRIFTS results shown in Figure 1, which demonstrate that HCHO is transformed to adsorbed DOM on $TiO_2$ mainly by consuming surface bridging OH groups (3674 $cm^{-1}$).

The DOM species is further oxidized via a dehydrogenation process, resulting in the formation of formate (HCOO) species. Three possible reaction pathways for the dehydrogenation of DOM species were calculated, including the transfer of an H atom to surface O species, surface OH, and another adsorbed DOM molecule (Figure 6). The transfer of an H atom from DOM to surface O species is calculated to be endothermic by 0.64 eV with an extremely high energy barrier of 1.95 eV (Figure 6a). The energy barrier of the dehydrogenation of DOM with one H atom transferring to an adjacent adsorbed DOM molecule to form an adsorbed $CH_3O$ species is predicted to be 1.32 eV (Figure 6b). Therefore, these two processes are prohibited under normal conditions. In contrast, the energy barrier for the dehydrogenation of DOM assisted by surface terminal OH is only 0.12 eV, much lower than assistance by surface O species or another adsorbed DOM molecule, and is easily surmountable at room temperature. Moreover, this process is exothermic by 2.12 eV (Figure 6c). Therefore, the dehydrogenation of DOM assisted by surface terminal OH is both thermodynamically and kinetically favorable, indicating that the formation of surface terminal OH species is beneficial for the transformation of DOM into formate ($CH_2O_2$ + t-OH → HCOO).

To understand the different behaviors of HCHO adsorption on Ir/$TiO_2$ and Pt/$TiO_2$, we also calculated the pathways of $H_2O$ dissociation on $TiO_2$ and also on Ir- and Pt-loaded $TiO_2$ (Figure S7 and Figure 7). On the pure $TiO_2$ (101) surface (Figure S7a), $H_2O$ dissociates into a terminal OH and bridging OH with a 0.48 eV energy barrier, but the dissociated state is obviously unstable. In contrast, a surface terminal OH tends to react with a bridge OH to form molecularly adsorbed $H_2O$ with only a 0.11 eV energy barrier (see the reverse process in Figure S7a). These results indicate that the adsorption of molecular $H_2O$ on $TiO_2$ is favorable.[43] After loading with Ir and Pt, there are two pathways for $H_2O$ dissociation on the catalyst surface. One is $H_2O$ dissociation into a terminal OH and a bridging OH on Ir/$TiO_2$ and Pt/$TiO_2$ with 0.49 and 0.41 eV energy barriers, but the energy of the dissociated state is still much higher than that of the initial state (Figure S7b,c). In the second pathway (Figure 7), $H_2O$ is dissociated into a terminal OH with an H atom captured by Ir or Pt with 0.86 and 0.57 eV energy barriers, and the energy of the dissociated state is almost identical to that of the initial state; therefore, the second pathway is more favorable on Ir/$TiO_2$ and Pt/$TiO_2$. These results show that the presence of Ir and Pt promote the

https://dx.doi.org/10.1021/acscatal.0c01901
ACS Catal. 2020, 10, 9706−9715

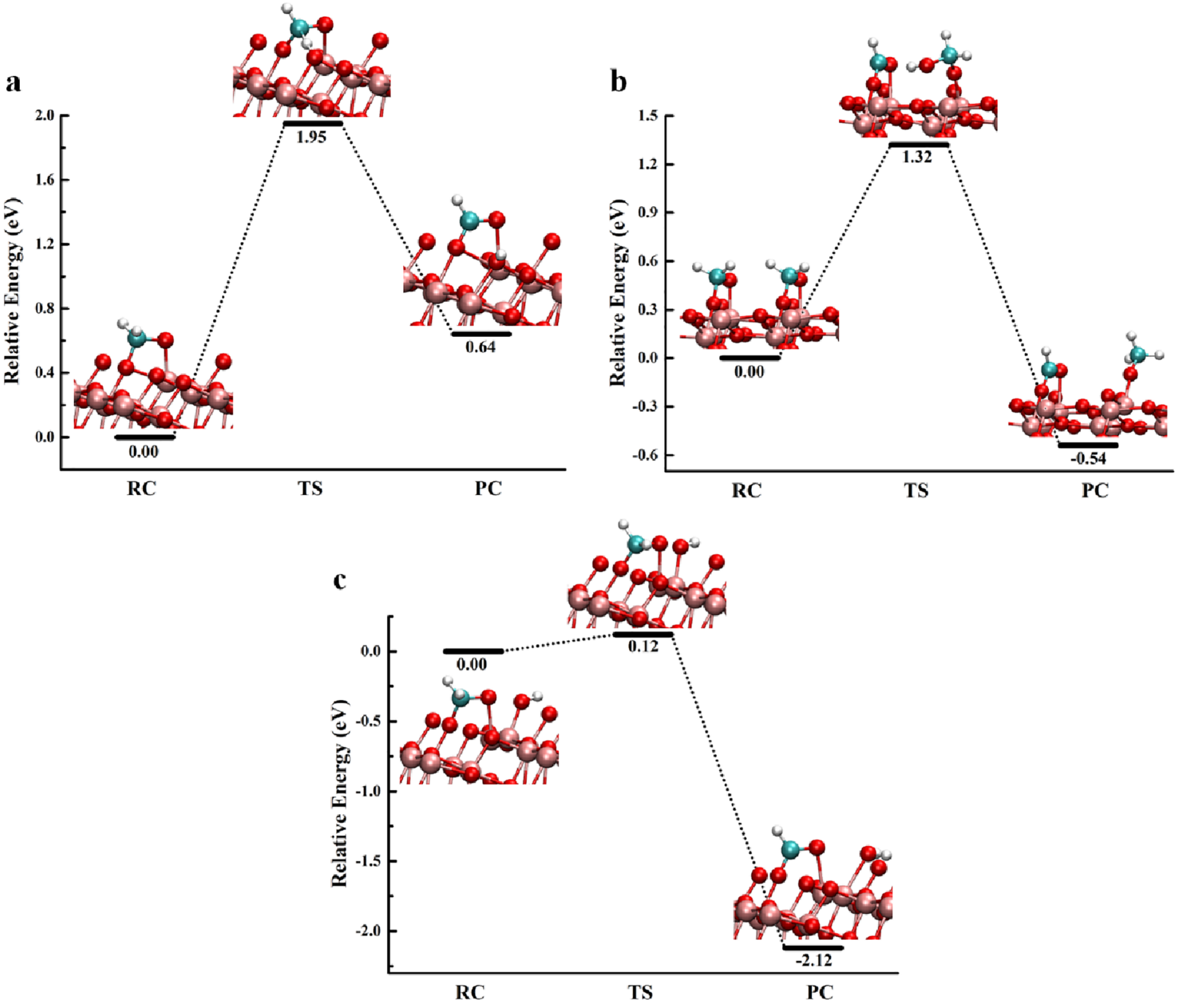

**Figure 6.** Energy profiles of the reaction pathway of (a) $CH_2O_2$ + Ti-O → HCOO + Ti-OH, (b) $CH_2O_2$ + $CH_2O_2$ → HCOO + $CH_3O$ + (Ti)-O, and (c) $CH_2O_2$ + Ti-OH → HCOO + Ti-$H_2O$ over anatase $TiO_2$ surfaces as well as the optimized geometries of the reactant, transition state, and product. Pink, red, cyan, and white circles denote Ti, O, C, and H atoms, respectively.

dissociation of $H_2O$ into surface terminal OH groups on $TiO_2$, and Pt is more active than Ir for $H_2O$ activation.

Based on the above results, we can clearly understand the different behaviors of HCHO transformation on $TiO_2$, Ir/$TiO_2$, and Pt/$TiO_2$. When HCHO adsorption takes place on $TiO_2$, HCHO consumes a bridging OH group to form DOM, and then, the H atom of the bridging OH group transfers to an adjacent terminal OH, producing molecularly adsorbed $H_2O$. Since pristine $TiO_2$ is not efficient for $H_2O$ dissociation into surface terminal OH, the DOM species cannot be further transformed and therefore are dominant on the $TiO_2$ surface. When Ir is loaded on $TiO_2$, $H_2O$ activation is promoted on Ir/$TiO_2$. Hence, the DOM species can further react with terminal OH to form formate species in the presence of $H_2O$ on Ir/$TiO_2$. Since Pt is more efficient than Ir for $H_2O$ dissociation, there should be more terminal OH groups available on the Pt/$TiO_2$ surface. Therefore, a large fraction of DOM is transformed into formate on Pt/$TiO_2$ during the HCHO adsorption process, and the formate species can further react with an OH group into final products in the presence of $H_2O$.

On the Ir/$TiO_2$ and Pt/$TiO_2$, $H_2O$ tends to dissociate into a terminal OH with an H atom captured by Ir or Pt. Hence, the H poisoning on Ir or Pt may exist following $H_2O$ dissociation. The H atoms on Ir or Pt may form $H_2$, participate in the activation of $O_2$ in the presence of $O_2$, or form protonated $H_2O$ ($H_3O^+$) in the presence of water vapor.[9,44−46] We tested the Pt/$TiO_2$ in a flow of $H_2O$ or $H_2O$ + HCHO and analyzed the products. There is no $H_2$ detected, indicating that the H atoms on Ir or Pt cannot form $H_2$. We previously have investigated the roles of $O_2$ and $H_2O$ in ambient HCHO oxidation on Ir/$TiO_2$ and Pt/$TiO_2$.[21,23] It is shown that both of $O_2$ and $H_2O$ are necessary for the reaction,[47] which requires the co-presence of $O_2$ and $H_2O$; otherwise, there will be no activity. In the absence of $H_2O$, since there is no source of active surface OH groups for HCHO oxidation, the catalyst shows no activity. In the absence of $O_2$, the deactivation of the catalyst may be due to the H atoms poisoning on Ir or Pt

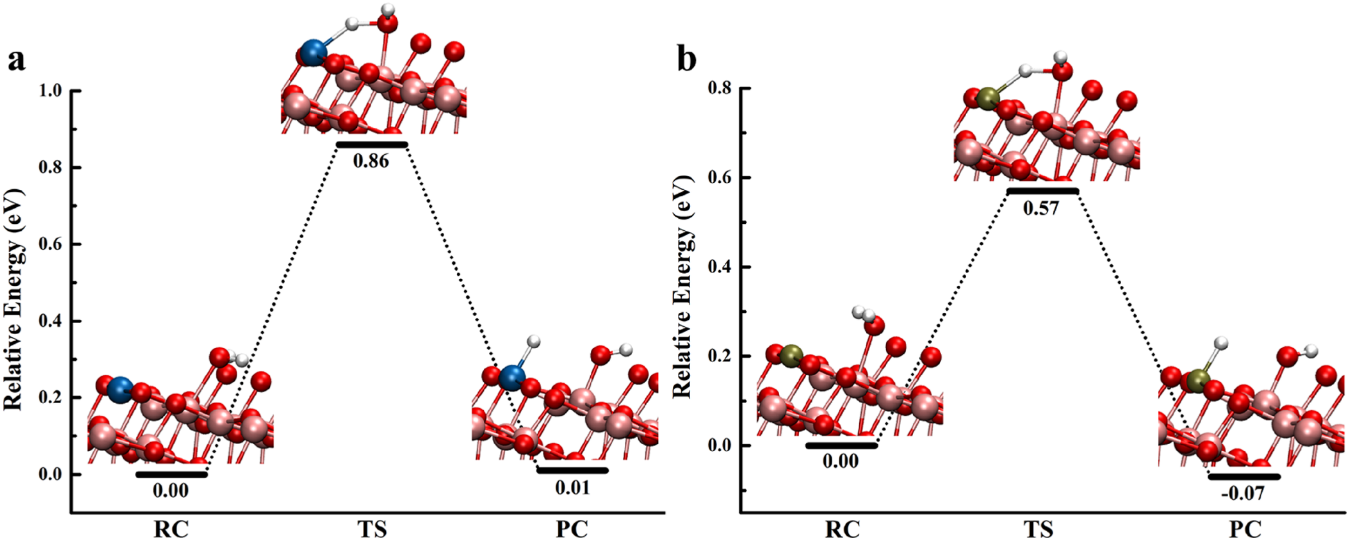

**Figure 7.** Energy profiles of the reaction pathway of $H_2O$ dissociation over (a) Ir/$TiO_2$ and (b) Pt/$TiO_2$ surfaces as well as the optimized geometries of the reactant, transition state, and product. Pink, red, cyan, white, ochre, and blue circles denote Ti, O, C, H, Pt, and Ir atoms, respectively.

during $H_2O$ dissociation. When $O_2$ is present, it can consume the H atoms and thereby avoid the H poisoning, facilitating the continuous activation of $H_2O$ and keeping the reaction going on.

## CONCLUSIONS

In this work, we investigated the influence of $O_2$ and $H_2O$ on HCHO adsorption and transformation on $TiO_2$, Ir/$TiO_2$, and Pt/$TiO_2$ using in situ DRIFTS and DFT calculations. We observe that the presence of $H_2O$ significantly improve the DOM transformation into formate species on $TiO_2$, and loading noble metals such as Ir or Pt onto $TiO_2$ dramatically promotes the activation of $H_2O$ to form surface terminal OH groups, therefore boosting the DOM transformation and even further conversion. We reveal that the bridging OH groups are involved in DOM formation, while the terminal OH groups are responsible for transformation of DOM into formate species and its further oxidation. The conversion of DOM into formate catalyzed by surface terminal OH groups has proven to be a facile pathway for DOM transformation. Our findings provide the new insights into the mechanism of HCHO transformation on metal oxide surfaces, which will definitely contribute to the deep understanding of the mechanisms of HCHO-related industrial catalytic reactions and also to the design of more efficient catalysts for HCHO oxidation.

## ASSOCIATED CONTENT

### Supporting Information

The Supporting Information is available free of charge at https://pubs.acs.org/doi/10.1021/acscatal.0c01901.

> Materials and methods; physical properties (Table S1); and structural formulas, XRD patterns, the anatase $TiO_2$ model used in the DFT calculation, in situ infrared dynamic spectra, FT-IR spectra, $NH_3$ adsorption spectra, and energy profiles (Figures S1−S7) (PDF)

## AUTHOR INFORMATION

### Corresponding Author

**Changbin Zhang** − *State Key Joint Laboratory of Environment Simulation and Pollution Control, Research Center for Eco-Environmental Sciences, Chinese Academy of Sciences, Beijing 100085, China; University of Chinese Academy of Sciences, Beijing 100049, China;* orcid.org/0000-0003-2124-0620; Email: cbzhang@rcees.ac.cn

### Authors

**Xueyan Chen** − *State Key Joint Laboratory of Environment Simulation and Pollution Control, Research Center for Eco-Environmental Sciences, Chinese Academy of Sciences, Beijing 100085, China; University of Chinese Academy of Sciences, Beijing 100049, China*

**Guangzhi He** − *State Key Joint Laboratory of Environment Simulation and Pollution Control, Research Center for Eco-Environmental Sciences, Chinese Academy of Sciences, Beijing 100085, China; University of Chinese Academy of Sciences, Beijing 100049, China;* orcid.org/0000-0003-1770-3522

**Yaobin Li** − *University of Chinese Academy of Sciences, Beijing 100049, China; Center for Excellence in Regional Atmospheric Environment, Institute of Urban Environment, Chinese Academy of Sciences, Xiamen 361021, China*

**Min Chen** − *State Key Joint Laboratory of Environment Simulation and Pollution Control, Research Center for Eco-Environmental Sciences, Chinese Academy of Sciences, Beijing 100085, China; University of Chinese Academy of Sciences, Beijing 100049, China*

**Xiaoxiao Qin** − *State Key Joint Laboratory of Environment Simulation and Pollution Control, Research Center for Eco-Environmental Sciences, Chinese Academy of Sciences, Beijing 100085, China; University of Chinese Academy of Sciences, Beijing 100049, China*

**Hong He** − *State Key Joint Laboratory of Environment Simulation and Pollution Control, Research Center for Eco-Environmental Sciences, Chinese Academy of Sciences, Beijing 100085, China; University of Chinese Academy of Sciences, Beijing 100049, China; Center for Excellence in Regional*

*Atmospheric Environment, Institute of Urban Environment, Chinese Academy of Sciences, Xiamen 361021, China*

Complete contact information is available at:
https://pubs.acs.org/10.1021/acscatal.0c01901

### Author Contributions

‖X.C. and G.H. contributed equally to this work.

### Notes

The authors declare no competing financial interest.

## ■ ACKNOWLEDGMENTS

This work was financially supported by the National Key R&D Program of China (2017YFC0211802), the Natural Science Foundation of China (21976196, 21707136, and 21906174), and the Youth Innovation Promotion Association of CAS (2019045).

## ■ REFERENCES

(1) Forzatti, P.; Tronconi, E.; Busca, G.; Tittarelli, P. Oxidation of Methanol to Methyl Formate over V-Ti Oxide Catalysts. *Catal. Today* **1987**, *1*, 209−218.

(2) Ai, M. The Reaction of Formaldehyde on Various Metal Oxide Catalysts. *J. Catal.* **1983**, *83*, 141−150.

(3) Cant, N. W.; Tonner, S. P.; Trimm, D. L.; Wainwright, M. S. Isotopic Labeling Studies of the Mechanism of Dehydrogenation of Methanol To Methyl Formate over Copper-Based Catalysts. *J. Catal.* **1985**, *91*, 197−207.

(4) Klier, K. Methanol Synthesis. *Adv. Catal.* **1982**, *31*, 243−313.

(5) Mazanec, T. J. On the Mechanism of Higher Alcohol Formation over Metal Oxide Catalysts: I. A Rationale for Branching in the Synthesis of Higher Alcohols from Syngas. *J. Catal.* **1986**, *98*, 115−125.

(6) Busca, G.; Lamotte, J.; Lavalley, J. C.; Lorenzelli, V. FT-IR Study of the Adsorption and Transformation of Formaldehyde on Oxide Surfaces. *J. Am. Chem. Soc.* **1987**, *109*, 5197−5202.

(7) Yang, P.; Pan, J.; Liu, Y.; Zhang, X.; Feng, J.; Hong, S.; Li, D. Insight into the Role of Unsaturated Coordination $O_2$c-$Ti_5$c-$O_2$c Sites on Selective Glycerol Oxidation over AuPt/$TiO_2$ Catalysts. *ACS Catal.* **2018**, *9*, 188−199.

(8) Torres, J. Q.; Royer, S.; Bellat, J.-P.; Giraudon, J.-M.; Lamonier, J.-F. Formaldehyde: Catalytic Oxidation as a Promising Soft Way of Elimination. *ChemSusChem* **2013**, *6*, 578−592.

(9) Wachs, I. E.; Madix, R. J. The Oxidation of $H_2CO$ on a Copper(110) Surface. *Surf. Sci.* **1979**, *84*, 375−386.

(10) Bowker, M.; Madix, R. J. XPS, UPS and Thermal Desorption Studies of the Reactions of Formaldehyde and Formic Acid with the Cu(110) Surface. *Surf. Sci.* **1981**, *102*, 542−565.

(11) Lavalley, J.-C.; Lamotte, J.; Busca, G.; Lorenzelli, V. Fourier Transform I.R. Evidence of the Formation of Dioxymethylene Species from Formaldehyde Adsorption on Anatase and Thoria. *J. Chem. Soc., Chem. Commun.* **1985**, 1006−1007.

(12) Li, S.; Lu, X.; Guo, W.; Zhu, H.; Li, M.; Zhao, L.; Li, Y.; Shan, H. Formaldehyde Oxidation on the Pt/$TiO_2$(101) Surface: A DFT Investigation. *J. Organomet. Chem.* **2012**, *704*, 38−48.

(13) Montoya, A.; Haynes, B. S. DFT Analysis of the Reaction Paths of Formaldehyde Decomposition on Silver. *J. Phys. Chem. A* **2009**, *113*, 8125−8131.

(14) Zhang, C.; He, H.; Tanaka, K.-i. Catalytic Performance and Mechanism of a Pt/$TiO_2$ Catalyst for the Oxidation of Formaldehyde at Room Temperature. *Appl. Catal., B* **2006**, *65*, 37−43.

(15) Kecskés, T.; Raskó, J.; Kiss, J. FTIR and Mass Spectrometric Studies on the Interaction of Formaldehyde with $TiO_2$ Supported Pt and Au Catalysts. *Appl. Catal., A* **2004**, *273*, 55−62.

(16) Shi, C.; Chen, B.-b.; Li, X.-s.; Crocker, M.; Wang, Y.; Zhu, A.-m. Catalytic Formaldehyde Removal by "Storage-Oxidation" Cycling Process over Supported Silver Catalysts. *Chem. Eng. J.* **2012**, *200-202*, 729−737.

(17) Senanayake, S. D.; Chong, S. V.; Idriss, H. The Reactions of Formaldehyde over the Surfaces of Uranium Oxides.: A Comparative Study between Polycrystalline and Single Crystal Materials. *Catal. Today* **2003**, *85*, 311−320.

(18) He, Y.; Ji, H. In-Situ DRIFTS Study on Catalytic Oxidation of Formaldehyde over Pt/$TiO_2$ under Mild Conditions. *Chin. J. Catal.* **2010**, *31*, 171−175.

(19) Chen, B.-B.; Shi, C.; Crocker, M.; Wang, Y.; Zhu, A.-M. Catalytic Removal of Formaldehyde at Room Temperature over Supported Gold Catalysts. *Appl. Catal., B* **2013**, *132-133*, 245−255.

(20) Idriss, H.; Kim, K. S.; Barteau, M. A. Surface-Dependent Pathways for Formaldehyde Oxidation and Reduction on $TiO_2$(001). *Surf. Sci.* **1992**, *262*, 113−127.

(21) Zhang, C.; Liu, F.; Zhai, Y.; Ariga, H.; Yi, N.; Liu, Y.; Asakura, K.; Flytzani-Stephanopoulos, M.; He, H. Alkali-Metal-Promoted Pt/$TiO_2$ Opens a More Efficient Pathway to Formaldehyde Oxidation at Ambient Temperatures. *Angew. Chem., Int. Ed.* **2012**, *51*, 9628−9632.

(22) Bai, B.; Li, J. Positive Effects of $K^+$ Ions on Three-Dimensional Mesoporous Ag/$Co_3O_4$ Catalyst for HCHO Oxidation. *ACS Catal.* **2014**, *4*, 2753−2762.

(23) Li, Y.; Chen, X.; Wang, C.; Zhang, C.; He, H. Sodium Enhances Ir/$TiO_2$ Activity for Catalytic Oxidation of Formaldehyde at Ambient Temperature. *ACS Catal.* **2018**, *8*, 11377−11385.

(24) Zhang, C.; He, H. A Comparative Study of $TiO_2$ Supported Noble Metal Catalysts for the Oxidation of Formaldehyde at Room Temperature. *Catal. Today* **2007**, *126*, 345−350.

(25) Huang, H.; Leung, D. Y. C.; Ye, D. Effect of Reduction Treatment on Structural Properties of $TiO_2$ Supported Pt Nanoparticles and Their Catalytic Activity for Formaldehyde Oxidation. *J. Mater. Chem.* **2011**, *21*, 9647−9652.

(26) Chen, X.; Chen, M.; He, G.; Wang, F.; Xu, G.; Li, Y.; Zhang, C.; He, H. Specific Role of Potassium in Promoting Ag/$Al_2O_3$ for Catalytic Oxidation of Formaldehyde at Low Temperature. *J. Phys. Chem. C* **2018**, *122*, 27331−27339.

(27) Zhang, Z.; Bondarchuk, O.; Kay, B. D.; White, J. M.; Dohnálek, Z. Imaging Water Dissociation on $TiO_2$(110): Evidence for Inequivalent Geminate OH Groups. *J. Phys. Chem. B* **2006**, *110*, 21840−21845.

(28) Vecchietti, J.; Bonivardi, A.; Xu, W.; Stacchiola, D.; Delgado, J. J.; Calatayud, M.; Collins, S. E. Understanding the Role of Oxygen Vacancies in the Water Gas Shift Reaction on Ceria-Supported Platinum Catalysts. *ACS Catal.* **2014**, *4*, 2088−2096.

(29) Kim, T. S.; Gong, J.; Ojifinni, R. A.; White, J. M.; Mullins, C. B. Water Activated by Atomic Oxygen on Au(111) to Oxidize CO at Low Temperatures. *J. Am. Chem. Soc.* **2006**, *128*, 6282−6283.

(30) Ojifinni, R. A.; Froemming, N. S.; Gong, J.; Pan, M.; Kim, T. S.; White, J. M.; Henkelman, G.; Mullins, C. B. Water-Enhanced Low-Temperature CO Oxidation and Isotope Effects on Atomic Oxygen-Covered Au(111). *J. Am. Chem. Soc.* **2008**, *130*, 6801−6812.

(31) Zhang, C.; Li, Y.; Wang, Y.; He, H. Sodium-Promoted Pd/$TiO_2$ for Catalytic Oxidation of Formaldehyde at Ambient Temperature. *Environ. Sci. Technol.* **2014**, *48*, 5816−5822.

(32) Liu, C.; Ma, Q.; He, H.; He, G.; Ma, J.; Liu, Y.; Wu, Y. Structure−Activity Relationship of Surface Hydroxyl Groups during $NO_2$ Adsorption and Transformation on $TiO_2$ nanoparticles. *Environ. Sci.: Nano* **2017**, *4*, 2388−2394.

(33) Liu, L. M.; McAllister, B.; Ye, H. Q.; Hu, P. Identifying an $O_2$ Supply Pathway in CO Oxidation on Au/$TiO_2$(110): A Density Functional Theory Study on the Intrinsic Role of Water. *J. Am. Chem. Soc.* **2006**, *128*, 4017−4022.

(34) Dutov, V. V.; Mamontov, G. V.; Zaikovskii, V. I.; Liotta, L. F.; Vodyankina, O. V. Low-Temperature CO Oxidation over Ag/$SiO_2$ Catalysts: Effect of OH/Ag Ratio. *Appl. Catal., B* **2018**, *221*, 598−609.

(35) Wang, F.; Ma, J.; He, G.; Chen, M.; Wang, S.; Zhang, C.; He, H. Synergistic Effect of $TiO_2$−$SiO_2$ in Ag/Si−Ti Catalyst for the

Selective Catalytic Oxidation of Ammonia. *Ind. Eng. Chem. Res.* **2018**, *57*, 11903−11910.

(36) Huang, H.; Leung, D. Y. C. Complete Oxidation of Formaldehyde at Room Temperature Using $TiO_2$ Supported Metallic Pd Nanoparticles. *ACS Catal.* **2011**, *1*, 348−354.

(37) Yang, T.; Huo, Y.; Liu, Y.; Rui, Z.; Ji, H. Efficient Formaldehyde Oxidation over Nickel Hydroxide Promoted Pt/$\gamma$-$Al_2O_3$ with a Low Pt Content. *Appl. Catal., B* **2017**, *200*, 543−551.

(38) Chen, M.; Ma, J.; Zhang, B.; Wang, F.; Li, Y.; Zhang, C.; He, H. Facet-Dependent Performance of Anatase $TiO_2$ for Photocatalytic Oxidation of Gaseous Ammonia. *Appl. Catal., B* **2018**, *223*, 209−215.

(39) Zhang, Y.; Chen, M.; Zhang, Z.; Jiang, Z.; Shangguan, W.; Einaga, H. Simultaneously Catalytic Decomposition of Formaldehyde and Ozone over Manganese Cerium Oxides at Room Temperature: Promotional Effect of Relative Humidity on the $MnCeO_x$ Solid Solution. *Catal. Today* **2019**, *327*, 323−333.

(40) Tsyganenko, A. A.; Filimonov, V. N. Infrared Spectra of Surface Hydroxyl Groups and Crystalline Structure of Oxides. *Spectrosc. Lett.* **2018**, *5*, 477−487.

(41) Wang, F.; He, G.; Zhang, B.; Chen, M.; Chen, X.; Zhang, C.; He, H. Insights into the Activation Effect of $H_2$ Pretreatment on Ag/$Al_2O_3$ Catalyst for the Selective Oxidation of Ammonia. *ACS Catal.* **2019**, *9*, 1437−1445.

(42) Lin, H.; Long, J.; Gu, Q.; Zhang, W.; Ruan, R.; Li, Z.; Wang, X. In Situ IR Study of Surface Hydroxyl Species of Dehydrated $TiO_2$: Towards Understanding Pivotal Surface Processes of $TiO_2$ Photocatalytic Oxidation of Toluene. *Phys. Chem. Chem. Phys.* **2012**, *14*, 9468−9474.

(43) Vittadini, A.; Selloni, A.; Rotzinger, F. P.; Grätzel, M. Structure and Energetics of Water Adsorbed at $TiO_2$ Anatase 101 and 001 Surfaces. *Phys. Rev. Lett.* **1998**, *81*, 2954−2957.

(44) Kim, J.-Y.; Lee, J. Kinetics, Mechanism, and Dynamics of the Gas-Phase H(D) Atom Reaction with Adsorbed D(H) Atom on Pt(111). *J. Chem. Phys.* **2000**, *113*, 2856−2865.

(45) Wang, J. G.; Hammer, B. Density Functional Theory Study of Water Dissociation in a Double Water Bilayer with or without Coadsorption of CO on Pt(111). *J. Chem. Phys.* **2006**, *124*, 184704−184707.

(46) Wang, J. G.; Hammer, B. Theoretical Study of $H_2O$ Dissociation and CO Oxidation on $Pt_2Mo$(111). *J. Catal.* **2006**, *243*, 192−198.

(47) Wang, X.; Rui, Z.; Ji, H. DFT Study of Formaldehyde Oxidation on Silver Cluster by Active Oxygen and Hydroxyl Groups: Mechanism Comparison and Synergistic Effect. *Catal. Today* **2020**, *347*, 124−133.